Optimized Load-Scheduling Algorithm for CubeSat's Electric Power System Management Considering Communication Link

BAYAN HUSSEIN , Graduate Student Member, IEEE
AHMED M. MASSOUD , Senior Member, IEEE
TAMER KHATTAB , Senior Member, IEEE
Qatar University, Doha, Qatar

CubeSats have been gaining significant interest as a cost-effective solution that can be built with low power requirements for different mission types. The most critical subsystem in CubeSats is the electrical power subsystem (EPS), which provides the required power to operate the remaining subsystems. This article presents an approach for optimizing load management and scheduling in CubeSat applications to ensure optimal coordination between the load demand, power generation, and energy storage while maintaining communication's quality of service requirements, namely the data rate and bit error rate (BER). The loads are divided into four types based on their priority. The load types are time-modulated, magnitude-modulated, time-and-magnitude-modulated, and fixed. An optimization problem is formulated with data rate and BER in the cost function while maintaining energy and power constraints. Multiple cases are investigated with different mission requirements. The solution obtained shows that the proposed scheduling algorithm meets the communication system's requirements while conserving power and energy resources.

Authors' addresses: B. Hussein, A. M. Massoud, and T. Khattab are with the Department of Electrical Engineering, Qatar University, Doha 2713, Qatar, E-mail: (bh1602414@qu.edu.qa; ahmed.massoud@qu.edu.qa; tkhattab@ieee.org) (*Corresponding author: Bayan Hussein.*)

I. INTRODUCTION

CubeSats have become increasingly attractive in the last few years because they offer a low-cost and low-power solution with faster wireless access and low latency levels [1]. CubeSats are a class of small satellites with a cubic shape. Thus, their optimized surface area maximizes their solar power generation [2]. They are typically deployed in low Earth orbit (LEO) and have a standard unit volume (U) of 10 cm $\times$ 10 cm $\times$ 10 cm and 1.33 kg mass [3]. CubeSats have multiple subsystems, as illustrated in Fig. 1, including the communication subsystem (COM), the on-board computer (OBC), the attitude and determination control subsystem (ADCS), and the electrical power subsystem (EPS), and the payload. The EPS is responsible for providing the electric energy from the solar energy to operate the remaining subsystems. It is designed to perform multiple tasks, namely electric power generation, conditioning, storage, and distribution [4]. The power generation is achieved by the photovoltaic (PV) panels attached to the CubeSat's sides. Deployable solar panels have been introduced to the design to further increase power generation. Power conditioning is achieved through power electronic converters that are included in the EPS, such as maximum-power-point trackers and voltage regulators. Moreover, the energy storage system—typically a battery pack— is for cases when solar energy is unavailable (i.e., eclipse cases) or the energy is insufficient. Power distribution modules are used to distribute the power to the different subsystems of the CubeSat. Thus, following the standard definitions of grid sizing and classifications, an interesting yet general mapping between grids and satellites can be created, and CubeSats can be considered as stand-alone/isolated dc nanogrids or microgrids (MGs), as shown in Fig. 2. Thus, in Table I, a classification of "space grids" is presented based on the standard conventional naming of terrestrial electrical grids [5], [6]. Because the operation of the CubeSat and the success of its mission highly depends on the power provided by the EPS, load management, known as demand-side-management, becomes a significant aspect to consider, primarily when the power availability is defined by variable conditions, such as the irradiance levels, temperature, and load conditions. Similar to MGs, the concept of dynamic loading can be adapted to allow scheduling based on the load type to enhance the load profile. The load types can be classified based on the CubeSat mission. Then, load scheduling can be implemented through a controller/algorithm that dictates the connection of the shiftable loads to the energy sources (solar panels/storage systems), i.e., clear ON/OFF operation. Alternatively, scheduling can be carried out by manipulating the levels of the supplied power to the controllable loads.

Unlike terrestrial power grids, load management in space power grids involves different goals besides cost and consumption minimization. An example is the quality of the communication between the CubeSat and the ground station. Quality requirements, such as the bit-error-rate (BER) and the communication link's data rate, become

| Terrestrial Power Grid	Power Requirements	Corresponding Space Power Grid	Power Requirements	Orbit	Typical Mass	Size in U	Satellite Category	Example
Macrogrids	> 300 kW	Large & Medium Satellites	> 500 W	GEO MEO LEO	> 500 kg	N/A	Large & Medium Satellites	International Space Station [7]
Minigrids	0.5-300 kW	Minisatellites	200-500 W	LEO	100-500 kg	> 12 U	Small Satellites	MagicBus by Redwire Space [8]
Microgrids	0.5-300 kW	Microsatellites	60-250W		10-100 kg	6-12 U		XB12 by Blue Canyon Technologies [9]
Nanogrids	10-500 W	Nanosatellites	10-60 W		1-10 kg	1-3 U		EPIC 1U by AAC Clyde Space [10]
Picogrids	< 10 W	Picosatellites	< 10 W		< 1 kg	0.25-0.5 U		ARCE-1 by IAE USF [11]
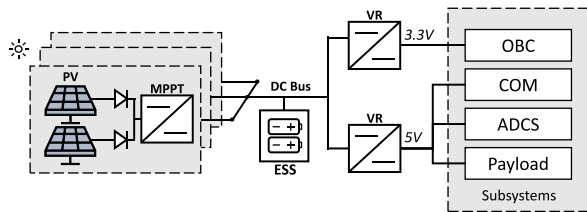
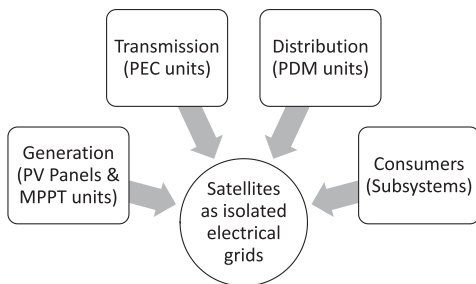Fig. 1.   EPS architecture in a CubeSat.

Fig. 2.   Components defining a satellite as a power grid.

essential when scheduling the CubeSats' subsystems and managing its power consumption. Moreover, adequate load management can also extend the lifetime of batteries since the charging and discharging processes are also optimized. Generally, many works in the literature focused on proposing load scheduling techniques in MGs, such as proactive and predictive controls considering operation cost and power flow to reduce stresses on MG [12], [13], dynamic network reconfiguration for economic and reliability objectives [14], and machine learning algorithms to provide more accurate results depending on the data availability [15], [16], [17].

Although most load scheduling solutions reported in the literature were proposed for MG applications, load scheduling for CubeSats has been considered. The early scheduling considerations were related to communication links, where the primary objective was to maximize communication time using linear programming algorithms [18]. In [19], a scheduling model was proposed using a genetic algorithm for job assembly. The model's only constraint was the operating time window, with no consideration for power and energy consumption. Later, scheduling algorithms began considering power and energy constraints in addition to the communication quality requirements. Such scheduling problems have been referred to as "Earth observing satellites scheduling problems." They included constraints related to power, thermal capacity, data capacity, and time [20], [21]. In addition to task scheduling, a task clustering technique was considered in [22]. Tasks with the same slewing angle and time duration were clustered together, and the scheduling problem was considered the priority of the task cluster. Since the task cluster could include a combination of critical and noncritical tasks, the scheduling model might not ensure power consumption by only critical loads during critical cases. In [23], an energy-driven scheduling model was proposed to maximize solar energy harvesting for nanosatellites and minimize power consumption. The maximization of solar energy was employed by dynamic control of task execution using load current control. Although the work considered energy constraints, it did not prioritize tasks/load, nor did it consider simultaneous task execution, which could reduce the efficiency of the scheduling model. Moreover, using a load current sensor for each load in the CubeSat would require larger areas, conflicting with the size and weight limitations. In [24], a state-space dynamic approach was used to optimize the execution of the task in an orbital cycle and calculate the state-of-charge (SoC) at the end of each cycle. Battery states were also considered to distinguish four modes of operation as normal, low power, safe, and emergency modes. The model only assumed a periodical load profile, which may not always be the case. Although the model prioritized the loads into critical, flexible, and scheduled loads, flexible loads were stochastically fed. In [25], a model predictive control was proposed for energy management in an aircraft's EPS to minimize load shedding. The model classified loads into only critical and noncritical loads. Moreover, although the authors in [24] and [25] considered task prioritization, they did not discuss the basis on which the tasks were classified. In [26], the proposed scheduling model aimed to offer a fault-tolerance capability to the CubeSat. The model only

considered the processors' queue and either accepted or rejected the task execution. The objective of the problem was to minimize the rejection rate considering reliability constraints. A demerit of this model is the possibility of data loss after task rejection, which may be unacceptable in some missions.

Load scheduling requires prioritization of tasks inside the CubeSat. Task, or load, classification has been lightly mentioned as an input to the model in some literature rather than discussing the classification's basis. Therefore, this work aims to achieve energy efficiency and system reliability by proposing a combination of mission-based load classification and load scheduling algorithms for CubeSat applications. The main contribution of this work can be summarized as follows.

1) A dynamic task classification technique where the task type can be altered during the mission. The task classification is conducted based on mission and communication requirements in terms of data rate and reliability (BER). The proposed load types are fixed, time-modulated (TM), magnitude-modulated (MM), and time-and-magnitude-modulated (TMM) loads.
2) The scheduling is performed on a daily basis by prioritizing task execution based on load type. The first priority is given to the fixed loads (FLs) in the CubeSat. The second priority is for MM loads, and the least priority is given to TM loads to allow some time for the battery to accumulate more energy.
3) For the highest reliability, time-modulated and TMM loads/tasks are preempted rather than rejected to prevent information loss of the rescheduled tasks. Moreover, MM loads/tasks are not necessarily postponed; instead, they are executed with a fraction of their rated power based on the power availability at that instant.
4) The scheduling model ensures that charging/discharging of the battery occurs in the linear region of the SoC-V curve, further enhancing battery health.

The rest of this article is organized as follows. Section II discusses the mission classification based on the communication requirements and the basis on which load types are classified. Then, Section III discusses the formulation of the optimization problem and the approach followed for reaching a feasible/optimal solution. Implementation and validation of the model are presented in Section IV. Finally, Section V concludes this article.

II. MISSION CLASSIFICATION AND LOAD SCHEDULING

A. Mission Requirements

The communication requirements and constraints can vary depending on the mission goal. As shown in Fig. 3, the first layer of the proposed classification criteria includes the following.
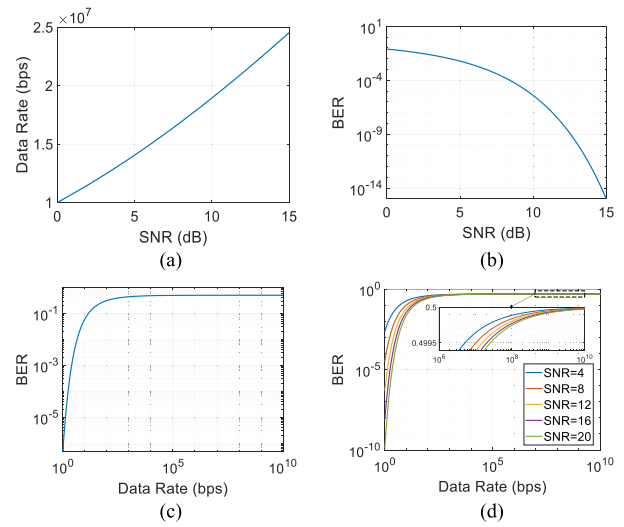

Fig. 3. Relation between (a) data rate and SNR, (b) BER and SNR, and (c) BER and data rate for BPSK modulation. (d) Family of BER and data rate curves for BPSK modulation.

1) The data rate R associated with the speed of transmission.
2) The reliability associated with the bit error rate BER.

These parameters are mapped into EPS considerations to form the second layer of the classification through the rate-power relation in (1), where it is assumed that the data rate approaches the channel capacity given by the Shannon–Hartley theorem

$$R = B \log_2 \left(1 + \text{SNR}_{\text{inst}}\right) \tag{1}$$

where R is the data rate (b/s), B is the channel bandwidth (Hz), and SNR_{inst} is the instantaneous signal-to-noise ratio given by

$$\text{SNR}_{\text{inst}} = \frac{P}{N} |h|^2 \tag{2}$$

where P and N are the signal and noise power, respectively, and $|h|^2$ is the channel power coefficient.

Moreover, the BER-power relation in (3) depends on many factors in the communication system, such as the modulation scheme and constellation. This work considers binary phase-shift keying (BPSK) modulation scheme for simplicity. The BER in BPSK is mathematically expressed as

$$\text{BER} = Q\left(\sqrt{2\gamma_b}\right) \tag{3}$$

where the Q function is defined as

$$Q(x) = \int_x^\infty e^{-\frac{x^2}{2}} \, dx \tag{4}$$

and γ_b is given as

$$\gamma_b = \frac{E_b}{N} \ |h|^2 = \frac{P}{NR}|h|^2 \tag{5}$$

where E_b is the bit energy (joules), N is the noise spectrum density (W/Hz), P is the signal power (W), R is the data rate (b/s), and $|h|^2$ is the channel power coefficient.
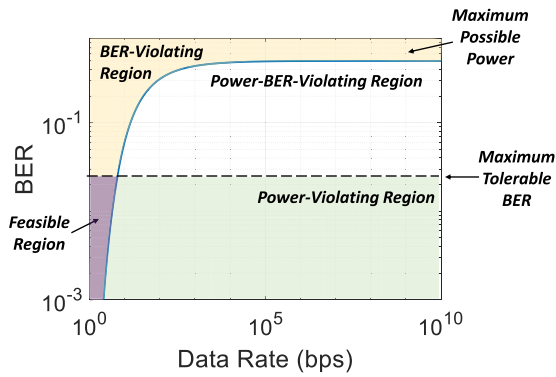
Fig. 4. Feasible operation region based on power and BER constraints.

Assuming that the noise power is constant for a given system, the relations in (1) and (3) illustrate the directly proportional (although nonlinear) behavior in the data rate and BER with the change in transmission power (represented by the SNR). This is graphically represented in Fig. 3(a) and (b), respectively. Moreover, the data rate is inversely related to reliability. For a given SNR, increasing the amount of data sent during a fixed duration increases the possibility that the receiver makes an error in a communication system, consequently increasing the BER. This can be seen in (5) and Fig. 3(c). A family of curves is shown in Fig. 3(d), showing how a change in SNR would affect the BER–rate curve. Setting the maximum acceptable BER and maximum possible power, the feasible operation region to meet these design constraints can be identified, as shown in Fig. 4. Finally, the energy considerations mainly depend on the operation duration and the power magnitude.

These three parameters (data rate, reliability, and power) are all coupled. Thus, for a given communication system, a compromise should be considered by fixing one of these parameters at a specific value, and the other two are calculated accordingly. Following up, four different general cases, as illustrated in Fig. 5, are distinguished for a CubeSat mission in terms of the communication system.

1) The communication system works with high data rates and demands high reliability. Since these two parameters are contradictory, the power needs to be high enough to satisfy both.
2) The communication system requires high data rates but is more tolerant of error (low-reliability requirements). In this case, the consumed power should be high to satisfy the data rate requirements.
3) The communication system works with low data rates but needs high reliability. In this case, a relatively smaller power can achieve the reliability requirement as per the inverse relation between the data rate and BER.
4) The communication system requires low data and low-reliability requirements. In this case, the consumed power is ultra-low, and there is complete flexibility in the power management in the CubeSat. Although this case is not typically practical, it is added to the classification for generalization.

In all these cases, the energy consumption mainly depends on the duration of the connection with the ground station (higher for longer operating periods). It is worth mentioning that these classifications can be further generalized based on the power consumption and operation duration not only for the communication system (Tx and Rx) but for every load inside the CubeSat. This includes the ADCS system, the payload, and all the tasks taking place on board.

B. Load Classifications

To efficiently design the EPS of a CubeSat, the mission requirements and loads on board are considered. Instead of discussing the load to the EPS as a constant one, the concept of dynamic loading is introduced to allow load scheduling. This section discusses the arrangement of loads to allow the scheduling based on the available power and energy provided by the EPS. The classification is considered in a time-magnitude domain, as shown in Fig. 6. Using this domain, new definitions are introduced to perform the scheduling and power management of loads. These definitions include the following.

1) TM loads are loads/tasks that can be shifted in time. In this category, the magnitude of the required power to perform the task is usually constant, but the urgency of the operation is not of high importance. Hence, the operation can wait until enough power is available. Time-modulating improves the load curve and manages the peak instances in CubeSat's load profile. This can be graphically represented, as shown in Fig. 6(a).
2) MM loads are loads/tasks whose power consumption can be controlled and altered based on the available power. In this category, the loads/tasks may have to occur simultaneously but with controllable power levels, as illustrated in Fig. 6(b).
3) TMM loads are loads/ tasks that can be both shiftable in time and controllable in magnitude. These are usually not urgent and can be considered supportive tasks rather than fundamental ones. This is shown in Fig. 6(c).
4) FLs are loads/tasks that need to take place at a given time and at a predefined power level that cannot be changed, as shown in Fig. 6(d). An example of this is the beacon signal. Sending the beacon signal is a prescheduled task performed to indicate the existence of the CubeSat and to report its health data to the ground station. Based on the operation and constraints of the mission, the beacon signal can either be transmitted in public (where any ground station can receive the signal) or private (where only the associated ground station can spot it). The beacon signal can be considered an FL in both cases because it is scheduled to be sent at a specific instant with a fixed data rate and reliability requirements.
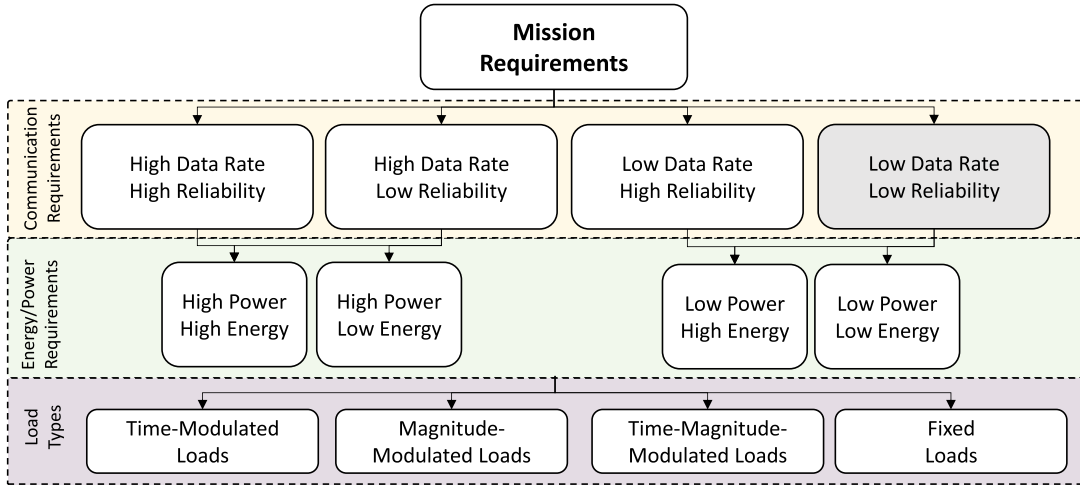
Fig. 5. Mission classification based on the communication requirements (the data rate and reliability) with the equivalent EPS requirements (power and energy) and the possible type loads.
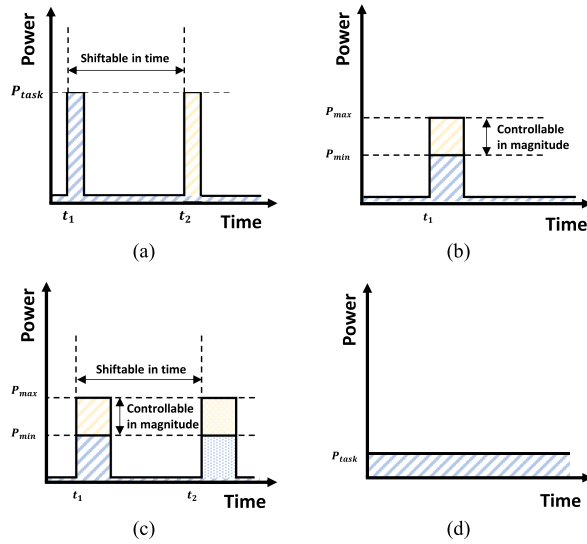

Fig. 6. Load types: (a) time-modulated, (b) MM, (c) TMM, and (d) fixed.

It should be noted that the same load can belong to different categories during different times in the mission, hence the concept of "dynamic loading."

III. SYSTEM DESCRIPTION AND PROBLEM FORMULATION

In this section, the system model is described. Based on the definitions, the constraints and objective functions of the optimization problem are constructed. The formulated problem is a combinatorial optimization problem [27].

A. System Model

Consider a CubeSat with M loads and a single generation source, i.e., PV panels. The goal is to schedule the loads in an optimal or near-optimal way during the whole day, which consists of F orbits, each having an orbital period T_{orb}. The sampling time T_s is defined as the smallest
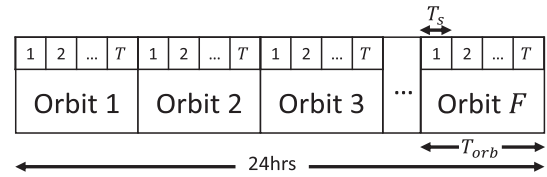

Fig. 7. Problem timeline and parameters.

change the scheduler can schedule over. Thus, as illustrated in Fig. 7, each orbital duration is divided into T slots. Then, the parameters F and T can be obtained by

$$F = \frac{24}{T_{\text{orb}}} \tag{6}$$

$$T = \frac{T_{\text{orb}}}{T_s}. \tag{7}$$

Moreover, the ith load can be represented as a vector of five quantities as

$$L_i = [a_i, b_i, d_i, p_i, y_i] \text{ for } i = 1, 2, \dots, M \tag{8}$$

where

$[a_i, b_i]$	interval in which load i can be turned ON;
d_i	duration for which the load has to be ON;
p_i	power rating of the load;
y_i	load type, i.e., FL, TM, MM, or TMM.

Let $u_i^{s,f}$ denote the status of the ith load at the sth time slot during the fth orbit in the day, the scheduling problem aims to find the set of the decision sequence u_i for load i laid out in a matrix form as

$$u_i = \begin{pmatrix} u_i^{1,1} & \cdots & u_i^{T,1} \\ \vdots & \ddots & \vdots \\ u_i^{1,F} & \cdots & u_i^{T,F} \end{pmatrix}, 0 \leq u_i^{s,f} \leq 1 \tag{9}$$

where each row denotes the status of the ith load at all time slots in a single orbit. Thus, u is a F by T by M decision matrix.

B. Constraints

To ensure that the power consumption is optimized and that the energy stored in the battery is not fully depleted, the constraints have to be power- and energy-dependent. The typical power consumed by all the loads in a CubeSat as a function of time, i.e., $P_{typ}(t)$, can be given as

$$P_{typ}(t) = \sum_{i=1}^{M} p_i. \tag{10}$$

The maximum demand (MD) at any time slot t, is expressed as

$$MD(t) = \max\left(P_{typ}(t)\right). \tag{11}$$

The scheduling problem aims to find the decision matrix u_i such that the total power at any time instant t does not exceed the predefined MD. From (10), the consumed energy by all loads in CubeSat at time t in terms of the decision variable is

$$E_{cons,i}(t) = \sum_{s=1}^{t}\sum_{i=1}^{M} p_i u_i^{s,f}. \tag{12}$$

The generated energy from the PV panels as a function of time is the accumulated power, and it is given by

$$E_{gen}(t) = \sum_{\tau=1}^{t}\left[\sum_{j=1}^{6} S_o \eta A \cos\left(\gamma(\tau)\right)\right] \tag{13}$$

where S_0 is the solar index of the orbit, η and A are the efficiency and area of the PV panel, respectively, γ is the incident angle of the Sun with the PV panel, and $j = 1, 2, \ldots, 6$ identifies the different faces of the CubeSat. In this work, it is assumed that the total generated energy can be calculated at any time instance as $\gamma(\tau)$ can be determined by CubeSat's ADCS. Finally, the energy stored in the battery can be given by

$$E_{bt}(t) = CV_{bt}(t) \tag{14}$$

where C is the battery capacity (Ah) and V_{bt} is the battery voltage (V).

C. Objective Function

The optimization problem aims to find the minimized cost function given in (15) that is a function of the following three objectives.

1) Maximizing the communication link data rate R.
2) Minimizing the communication BER.
3) Minimizing the total consumed energy by all Cube-Sat loads.

$$c = \omega_1 f_1 + \omega_2 f_2 + \omega_3 f_3. \tag{15}$$

The weights ω_1, ω_2, and ω_3 can be freely tuned based on the requirements and needs of the mission, and the three objectives are as follows:

$$f_1 = \frac{1}{R} \tag{16}$$

$$f_2 = BER = Q\left(\sqrt{2\frac{x}{NR}}\right) \tag{17}$$

$$f_3 = E_{cons} = \sum_{i=1}^{M}\sum_{f=1}^{F}\sum_{s=1}^{T} p_i u_i^{s,f} \tag{18}$$

with x being the instantaneous SNR by the CubeSat's COM system

$$x = |h|^2 \sum_{f=1}^{F}\sum_{s=1}^{T} p_i u_i^{s,f} \text{ for } i = COM. \tag{19}$$

D. Optimization Problem

Assuming that CubeSat's mission is communication-based, two main quality requirements have to be ensured: data rate and BER. Thus, ω_3 can be set to 0 in (15). The formulated optimization problem with the previously discussed constraints can be expressed as

Obj. fcn.:

$$\text{Minimize } c = \omega_1 f_1 + \omega_2 f_2 \tag{20}$$

subject to:

$$R\sum_{f=1}^{F}\sum_{s=1}^{T} u_i^{s,f} = I, i = COM \tag{21}$$

$$p_i u_i^{s,f} \leq MD_i \text{ at } a_i \leq t \leq b_i$$
$$i = 1, 2, .., M \tag{22}$$

$$u_i^{s,f} = 0 \text{ at } a_i > t > b_i, i = 1, 2, .., M \tag{23}$$

$$E_{cons}(t) \leq E_{bt}(t) + E_{gen}(t) \tag{24}$$

$$f_2 \leq BER_{max} \tag{25}$$

$$R_{min} \leq R \leq B\log_2(1 + x) \tag{26}$$

$$0 \leq u_i^{s,f} \leq 1. \tag{27}$$

The first constraint in (21) is relevant to the COM system, ensuring that the total amount of data in bits I should be transmitted to the ground station. The constraint in (22) ensures that the actual power consumption of each load during its operational time does not exceed the load's predefined MD. The constraint in (23) ensures that the loads are not turned ON outside their permissible limits. The energy constraint in (24) ensures that the actual consumed energy at any time slot t does not exceed the generated and stored energies from the PV panels and in the battery, respectively. The constraint in (25) ensures that the data rate is higher than the minimum required rate and less than the channels' capacity, given by the Shannon–Hartley limit. Moreover, the constraint in (26) ensures that the BER is less than the maximum acceptable BER. Finally, the constraint in (27) is a relaxation constraint that allows magnitude modulation instead of strictly ON/OFF results.

IV. IMPLEMENTATION RESULTS AND DISCUSSION

The previous works on CubeSat's EPS management mainly focus on either the power/energy considerations or the communication window. The inclusion of both the

power/energy constraints and communication link requirements is crucial as it provides a way to increase the efficiency and performance of CubeSat, such that not only the power is adequately-managed and the battery health is improved, but also the performance of the communication system is enhanced via the consideration of the data rate and the BER. The data rate and BER are typically constrained by specific and predefined quality limits. However, in this work, it is intended to optimize both parameters. This is achieved by classifying the loads into time-modulated, MM, TMM, and FLs. With such classification, each load can be classified based on power/energy availability without jeopardizing the communication link quality constraints.

The previously discussed minimization problem model is implemented in MATLAB using the problem-based optimization approach. The implementation is conducted for a full day, assuming a deterministic channel representation. The following sections discuss the details and considerations of channel representation, loads and system parameters, results, and discussion.

A. Deterministic Channel Representation

The channel power coefficient is crucial in calculating the instantaneous SNR and thus accurately computes the channel capacity and BER given in (1) and (3). Channel power gain is essentially the ratio between the received and transmitted power signal power. This work assumes that the wireless communication channel between the CubeSat and the base station follows a deterministic free space path loss (FSPL) law. The involvement of FSPL in the optimization problem is crucial to ensure enough power is supplied to the COM to reach the receiver. Starting with the Friis transmission formula, the FSPL is calculated by

$$\text{FSPL}(d) = \frac{P_t}{P_r} = \left(\frac{4\pi d}{\lambda}\right)^2 = \left(\frac{4\pi f}{c}d\right)^2 \quad (28)$$

where λ is the signal wavelength (m), d is the distance between the antennas (m), f is the signal's frequency (Hz), and c is the speed of light (3×10^8 m/s).

To compute the FSPL deterministically, the distance between the CubeSat and the base station antennas can be represented as a function of the elevation angle given by [28]

$$d(\varepsilon) = R_e \sqrt{z^2 - \cos^2 \varepsilon} - R_e \sin \varepsilon$$
$$\text{where } z = \frac{H + R_e}{R_e} \quad (29)$$

where R_e is the Earth's radius (m), H is the LEO orbit's altitude from the Earth's surface (m), and ε is the elevation angle (rad), which is the angle between the line connecting the two antennas and the Earth's tangent.

Assuming that the CubeSat starts orbiting the Earth directly above the base station, the elevation angle ε is computed as a function of time as

$$\varepsilon(t) = \frac{2\pi}{T_{\text{orb}}} t + \frac{\pi}{2}. \quad (30)$$

TABLE II
Implementation Parameters

Loads	Number of FL	4
	Number of TMM loads	1
Orbit	Orbital Period, T_{orb}	120 mins
	Sampling time, T_s	2 mins
	Time steps per orbit, T	60 steps/orb
	Orbits per day, F	12 orb/day
Battery	Maximum Voltage	8 V
	Minimum Voltage	6 V
	Battery Capacity	5 Ah
Communication Link and Channel	Channel Representation	FSPL
	Frequency Band	VHF
	Channel Bandwidth, BW	20 kHz
	Noise Power, N	-132.6 dBm

Finally, the channel power coefficient is given as

$$|h|^2 = \frac{P_r}{P_t} = \frac{1}{\text{FSPL}}. \quad (31)$$

B. Loads and System Parameters

In this work, the approach followed is to consider the COM system as a TMM load, where its duration varies depending on the data rate value. The EPS, OBC, ADC, and payload are considered FL, as shown in (8).

$$L_{\text{com}} = [60, 300, -, 4.4, \text{TMM}]$$
$$L_{\text{eps}} = [1, 720, 720, 0.4, \text{FL}]$$
$$L_{\text{obc}} = [1, 720, 720, 0.75, \text{FL}]$$
$$L_{\text{adc}} = [1, 720, 720, 1.4, \text{FL}]$$
$$L_{\text{payload}} = [1, 10, 10, 1.45, \text{FL}]. \quad (32)$$

It is assumed that the orbital period is $T_{\text{orb}} = 120$ min and the sampling time is $T_s = 2$ min. Thus, the number of orbits per day is $F = 12$ orb/day, and the total time steps for an orbital period are $T = 60$ slots/orb. The scheduling algorithm is performed at the beginning of the period. Table II presents the constants' values assumed in the simulation. Assuming a mission capturing a picture of a land, the camera payload should operate at a specific instant (FL). However, to add flexibility to the mission and meet the energy constraints within the CubeSat, the picture can be sent to the ground station at the optimal scheduled time to ensure that it meets the communication reliability conditions of higher data rates and lower BER with lower energy consumption levels, based on the channel condition and EPS energy availability.

Assuming that the average total power generated in the CubeSat is 10 W, the MD for the COM at any time can be computed by eliminating the portion spent on the FLs

$$\text{M D}_{\text{com}} = 10 - \sum_i p_i, \; i \neq \text{COM} \quad (33)$$
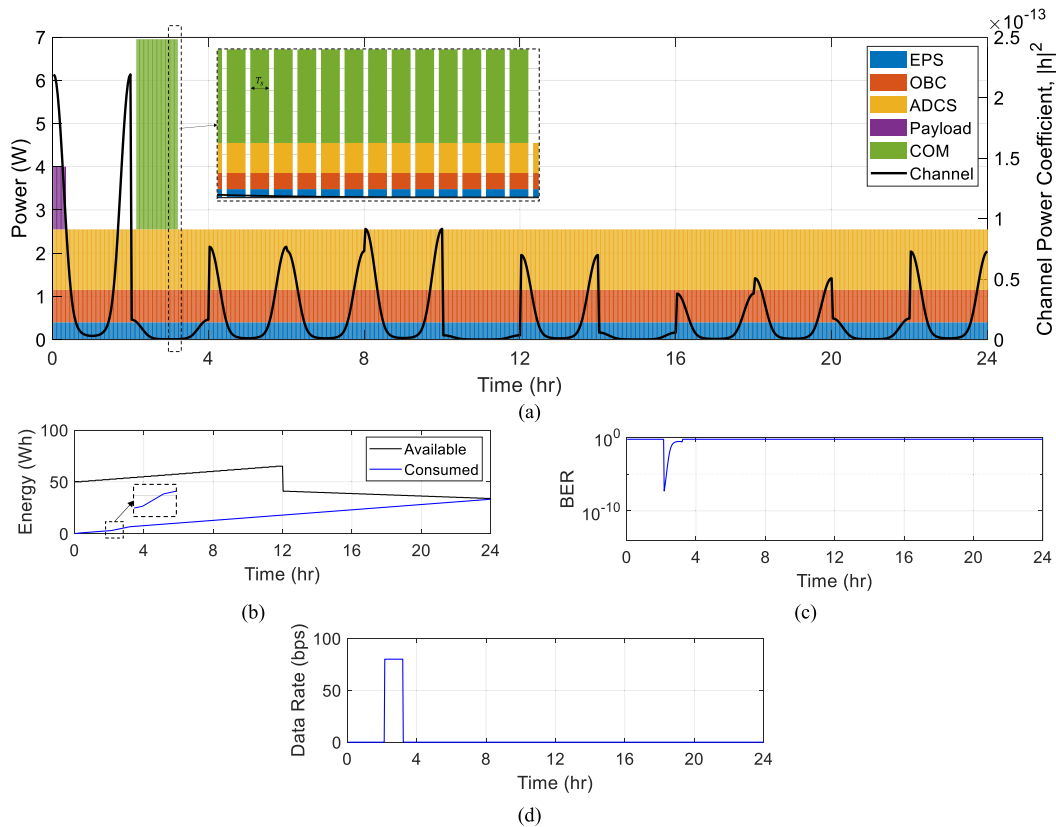
where p_i is the power demand for the ith load.

Fig. 8. Base case. (a) Load versus channel power gain condition. (b) Available and consumed energy profile. (c) BER profile. (d) Data rate profile.

C. Implementation Considerations

This section demonstrates implementing the previously discussed optimization problem in MATLAB's Optimization Toolbox using the problem-based approach. This work has the following assumptions.

1) The transmission is performed in the very-high-frequency (VHF) band, with 20-kHz bandwidth and a -132.6 dB noise level [28].
2) The total available energy profile, essentially the PV-generated energy and battery-stored energy, is provided to the scheduler as input data. The profile consists of two main regions: the first is the sunlit period, where the solar energy is increasing, and the battery energy is accumulating. The second region is the eclipse period, where solar generation is stopped, and the CubeSat operates by energy stored in the battery. The discharging of the battery is constrained in the linear region to improve the battery health, where the minimum and maximum voltages are 6 V and 8 V, respectively.
3) The deadlines of the communication window, i.e., $[a_{com}, b_{com}]$ are not necessarily dependent on the energy profile. Instead, they are specified by the mission operator and are provided to the scheduler as input.
4) The channel power coefficients are calculated by (31).

5) The CubeSat has loads as given in (32).

With these assumptions, the following cases are implemented.

1) *Base Case:* In this case, no scheduling is performed, and the COM transmission occurs with full rated power to transmit $I = 0.3$Mb with and data rate $R = 80$b/s. The schedule of this case is presented in Fig. 8(a). Since the channel condition is not considered, power is provided to the COM transmitter even in poor channel conditions. This only consumes the available energy without actively transmitting data since the location of the CubeSat is not in the base stations' line of sight. The energy resources are not well-utilized because the channel condition is not considered. Moreover, Fig. 8(b) shows the energy and BER profiles. The BER values are relatively higher during the communication window at instants when the channel condition is poor because the instantaneous SNR is low.

2) *Load Scheduling:* In this case, the scheduling process is optimized to send a fixed amount of data with the aim of data rate maximization and BER minimization. The cost function weights are set as $\omega_1 = \omega_2 = 1$. The obtained solution shows a data rate $R = 144.6$ b/s to send 0.3 Mb of data, with the lowest BER of 3.40×10^{-17}. These results show an increased data rate and reduced BER compared to the base case. The resulting load schedules are presented in Fig. 9(a), with energy, BER, and data rate profiles shown in Fig. 9(b). Compared with Fig. 8(b), the sudden increase in
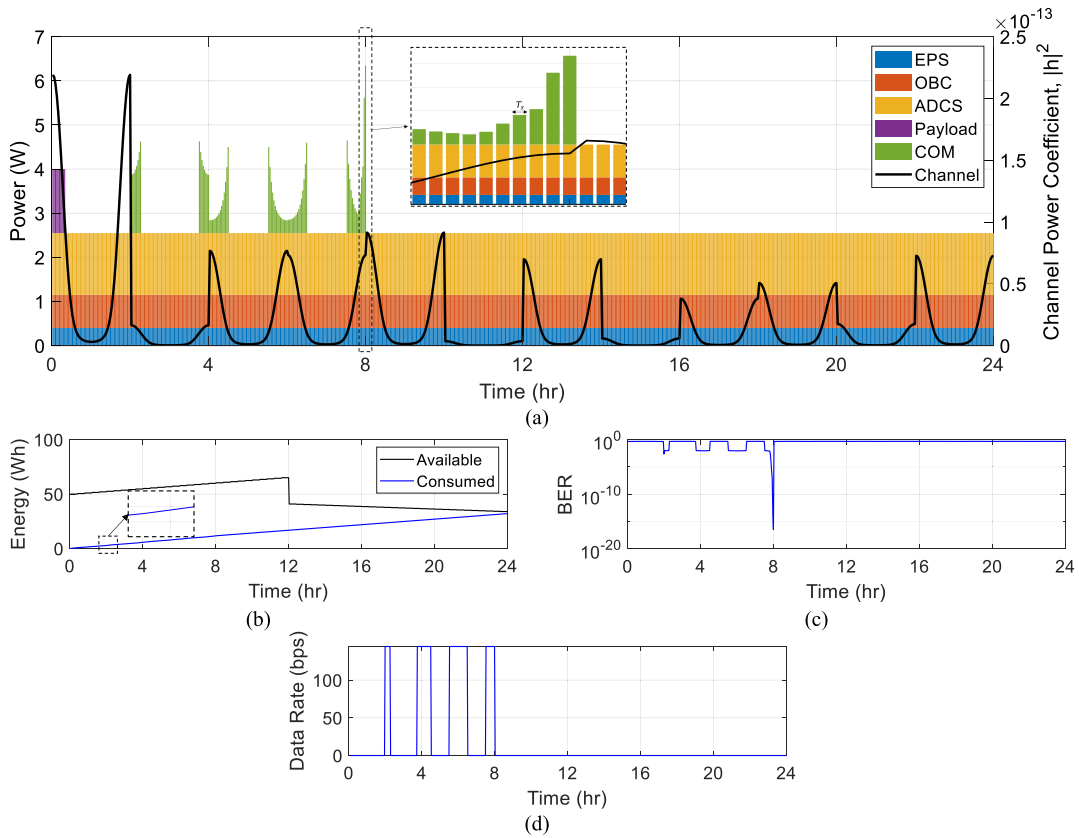
Fig. 9. Load scheduling with a fixed amount of data and $\omega_1 = \omega_2 = 1$. (a) Optimized load schedule versus channel power gain condition. (b) Available and consumed energy profile. (c) BER profile. (d) Data rate profile.

the energy in the base case is now minimized in Fig. 9(b) because of the MM load. Generally, in BER profiles, the lowest BER values occur during the peak power within the communication window, i.e., when the channel condition is high. When the channel condition is poor, the BER approaches 0.5, and no amount of power can enhance the BER. Communication during such instances is ineffective as the probability of the correct bit reception receiver is 50%, meaning the receiver is simply guessing information. Thus, the COM load is turned OFF at poor channel conditions to avoid wasting energy.

D. Priority Considerations

Optimization of load schedules for a fixed amount of data yields almost similar data rate values. To investigate the priority considerations and the effect of the cost function weights on the obtained solutions, the constraint in (21) is relaxed into a range. The appropriate priority weights are typically chosen based on the mission requirements. That is, if the mission requires high- reliability communication and has zero tolerance for error, full priority is given to minimizing the BER. On the other hand, if the main requirement of the mission is achieving higher data rates, full priority is given to the maximization of the data rate (minimization of $f_1 = 1/R$). Given a CubeSat mission, it is typically expected that both the data rate and BER are important. Thus, partial priorities are considered where more weight

is given to a specific parameter than the other. The different implemented scenarios are showcased in Fig. 10.

1) *Full Priority Scenario:* In this scenario, the data rate or the communication's reliability takes full priority without considering the other parameter. The following two cases are considered.

Case I: In this case, reliability is of utmost concern, and thus full priority is given to f_2 minimization, i.e., with cost function weights as $\omega_1 = 0$ and $\omega_2 = 1$. The results of this case yield a data rate of rate $R = 50.3$ b/s with load schedules shown in Fig. 11(a). Moreover, the energy, BER, and data rate profiles are shown in Fig. 11(b). The power and energy constraints are met, and the lowest BER is 2.91×10^{-19} at the instant corresponding to peak power (peak SNR).

Case II: This corresponds to the other extreme case, where full priority is given to f_1 minimization (data rate maximization). In this case, the cost function weights are set as $\omega_1 = 1$ and $\omega_2 = 0$. The obtained solution sets the data rate $R = 113.7$ b/s with the load schedule shown in Fig. 12(a). Accordingly, the energy, BER, and data rate profiles are shown in Fig. 12(b). Since the reliability requirement is low, the power levels given to the COM are low during the communication window, causing the lowest BER to be 3.1×10^{-7}.

By comparing these two extreme cases, the choice of the cost function weights, ω_1 and ω_2, reflects the priority
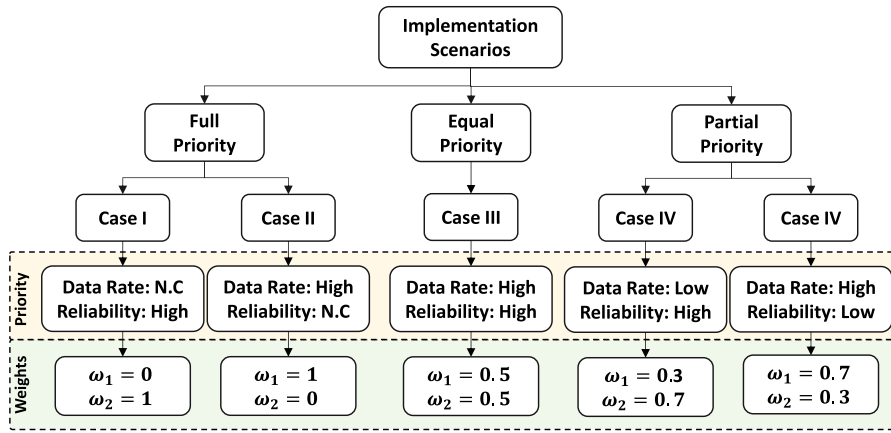
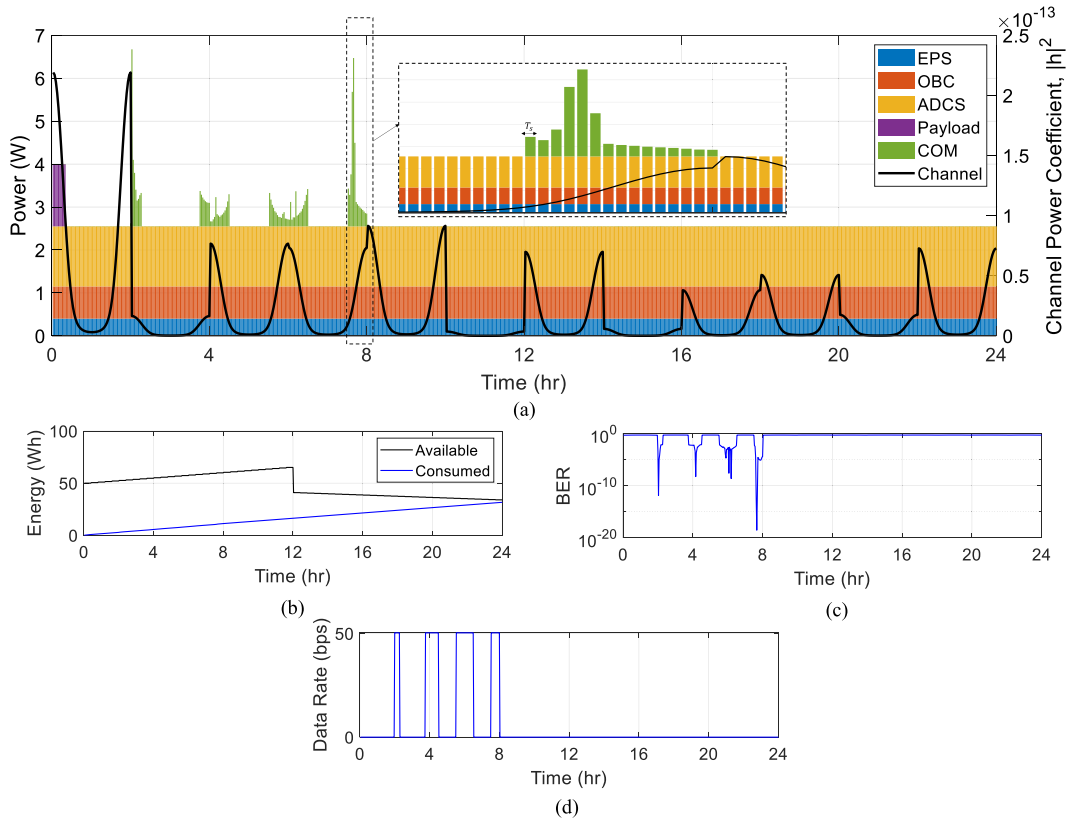Fig. 10. Summary of implemented cases (N.C: Not Considered).

Fig. 11. Case I: Full priority for f_2 minimization with $\omega_1 = 0$ and $\omega_2 = 1$. (a) Optimized load schedule versus channel power gain condition. (b) Available and consumed energy profile. (c) BER profile. (d) Data rate profile.

of the communication requirements. This is evident in the obtained results, where the data rate is increased when ω_1 is increased, and the BER is increased when ω_2 is reduced. Generally, since the concept of MM is introduced to the system, partial power is given to the COM system during the strong-channel instants to send the required data to the base station, whereas lower power levels are given during poor channel conditions.

2) *Equal Priority Scenario:* In this scenario, the minimization cost function has equal weighting parameters for both f_1 and f_2 with $\omega_1 = \omega_2 = 0.5$.

Case III: Both communication speed and reliability are required. Since the data rate maximization and BER minimization are inversely related, a compromise shall be found with respect to the channel condition, information amount, transmission deadlines, power, and energy constraints. The optimization output for this case shows that $R = 106.5$ b/s, and the schedules are shown in Fig. 13(a). The energy, BER, and data rate profiles are shown in Fig. 13(b). The lowest BER profile is 3.97×10^{-7}.

Comparing this case with the previous two, choosing the cost function weights evidently impacts the obtained
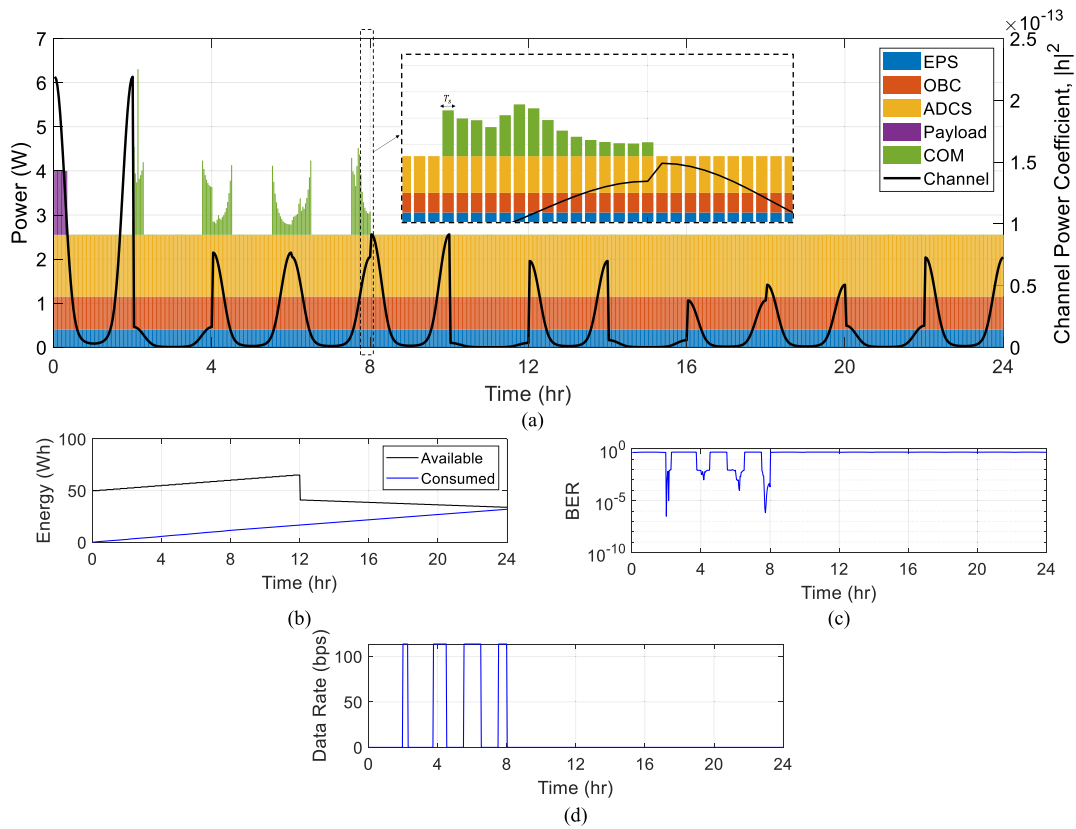
Fig. 12. Case II: Full priority for f_1 minimization (data rate maximization) with $\omega_1 = 1$ and $\omega_2 = 0$. (a) Optimized load schedule versus channel power gain condition. (b) Available and consumed energy profile. (c) BER profile. (d) Data rate profile.
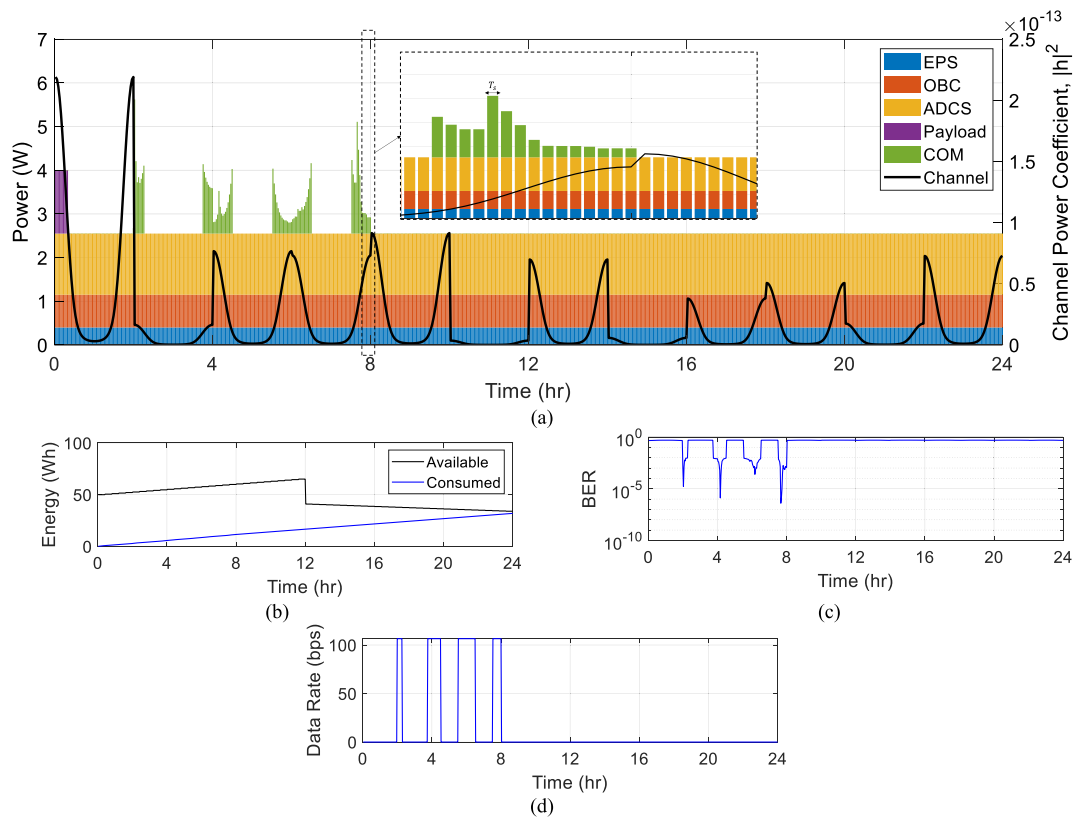

Fig. 13. Case III: Equal priority case with $\omega_1 = \omega_2 = 0.5$ (a) Optimized load schedule versus channel power gain condition. (b) Available and consumed energy profile. (c) BER profile. (d) Data rate profile.
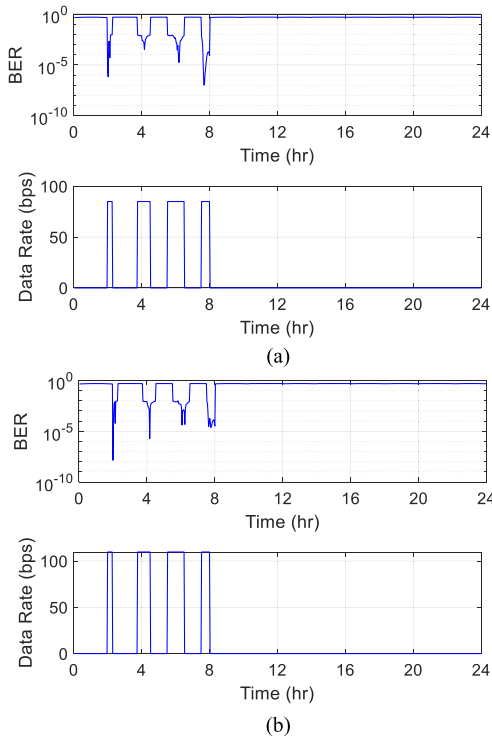
Fig. 14. BER and data rate profiles for partial priority cases. (a) Case IV: $\omega_1 = 0.3$ and $\omega_2 = 0.7$. (b) Case V: $\omega_1 = 0.7$ and $\omega_2 = 0.3$.

Fig. 15. Feasible region with power, rate, and BER constraints.

results. First, the obtained data rate is higher than the first case but lower than the second case.

3) *Partial Priority Scenario:* This scenario allocates higher priority to one of the parameters (data rate and BER) than the other without completely disregarding it. The following two cases are considered.

Case IV: In this case, a higher priority is given to BER minimization, with cost function weights as $\omega_1 = 0.3$ and $\omega_2 = 0.7$. The results of this case yield a data rate of rate $R = 85$ b/s. Moreover, the BER profile shown in Fig. 14(a) shows that the lowest achieved BER is 1.03×10^{-7}, which is relatively lower compared with cases II and III.

Case V: In this case, a higher priority is given to communication speed over reliability; thus, more weight is given to f_1 minimization (data rate maximization). The cost function weights are set as $\omega_1 = 0.7$ and $\omega_2 = 0.3$. The obtained solution sets the data rate $R = 109.7$ b/s, which is significantly higher than cases I, III, and IV because of the choice of weight. Moreover, the lowest BER in the profile shown in Fig. 14(b) is 1.42×10^{-8}.

Comparing these two cases and the other cases, the obtained values for the data rate and BER are significantly impacted by the cost function weights. Thus, based on the mission communication requirements, the load schedules can be generated.

E. Discussion Remarks

The previous section presented the implementation results for multiple scenarios with different weighting factors,
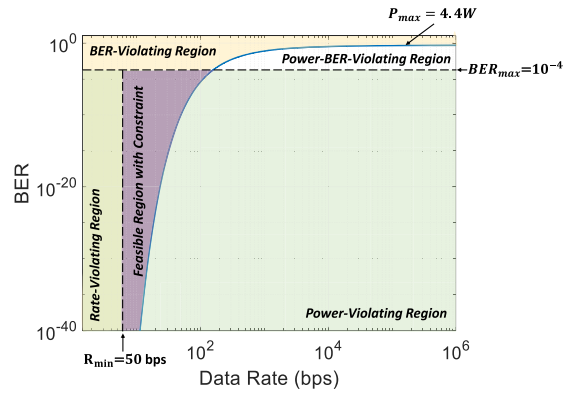
representing the priorities of the communication link requirements. In Table III, the implementation results for the five cases and the base case are summarized and organized to visualize the effect of the cost function weight choice and the communication link requirements. The results are given in terms of the achieved data rate, lowest BER, transmitted data, and the energy consumed by the COM system. It shall be noted that the amount of transmitted data is directly proportional to the obtained data rate. Moreover, in the implemented scenarios, the obtained data rate values are noticeably low because the feasible region in this problem—which is the area enclosed by the boundaries $R_{\min}$, $\text{BER}_{\max}$, and the BER–rate curve that is impacted by $P_{\max}$—is narrow, as shown in Fig. 15, where there is no room for a high data rate with the required maximum tolerable BER, i.e., $\text{BER}_{\max}$. In other words, relaxing the value of $\text{BER}_{\max}$ into a lower value can result in relatively higher data rate values and correspondingly higher amounts of transmitted data, as illustrated in cases in Table IV. Moreover, in all cases, the power consumed by the COM subsystem is lower than the base case because of the magnitude-modulation concept. The average energy consumed by the COM system is almost similar in all cases. The main difference is the tradeoff between the link data rate and the BER, which mainly depends on the choice of the cost function weights. Generally, the BER profile depends on the COM operating instances, where BER is the lowest when more power is given to the COM system, and this corresponds to the time instants where the channel power coefficient is high, i.e., when the CubeSat is closer to the base station. In superior-channel scenarios, a lower power magnitude is given to the COM system. Adversely, higher power magnitude is supplied to COM to compensate for the relatively poor channel instances, as shown in Figs. 9(a), 12(a), 13(a), and 14.

Increasing the data rate also increases the BER, which is undesirable. This is demonstrated in case III (compared with case II), where the lower data rate resulted in a reduced (improved) BER profile. Also, in case V (compared to case IV), the higher data rate results in increased (worse) BER. Addressing this issue, one way to have high data rates and acceptable BER profile is using other M-ary modulation

TABLE III
Summary of Implemented Cases

Case	Cost Function Weights		Obtained Data Rate	Lowest Achieved BER	Approximate Transmitted Data	COM's Energy Consumption
	$f_1 = 1/R$	$f_2 = BER$				
Base Case	N/A	N/A	80 bps	4.96×10^{-8}	0.31×10^6 bits	2.3467 Wh
Scheduling	$\omega_1 = 1$	$\omega_2 = 1$	144.6 bps	3.40×10^{-17}	0.30×10^6 bits	1.2680 Wh
Priority Considerations						
Case I	$\omega_1 = 0$	$\omega_2 = 1$	50.3 bps	2.91×10^{-19}	0.0656×10^6 bits	0.7979 Wh
Case IV	$\omega_1 = 0.3$	$\omega_2 = 0.7$	85 bps	1.03×10^{-7}	0.1378×10^6 bits	0.9905 Wh
Case III	$\omega_1 = 0.5$	$\omega_2 = 0.5$	106.5 bps	3.97×10^{-7}	0.1897×10^6 bits	1.0880 Wh
Case V	$\omega_1 = 0.7$	$\omega_2 = 0.3$	109.7 bps	1.42×10^{-8}	0.2061×10^6 bits	1.1476 Wh
Case II	$\omega_1 = 1$	$\omega_2 = 0$	113.7 bps	3.1×10^{-7}	0.2153×10^6 bits	1.1576 Wh

TABLE IV
Summary of Implemented Cases After Relaxing the Value of BER_{max}

Case	Cost Function Weights		Obtained Data Rate	Lowest Achieved BER	Approximate Transmitted Data	COM's Energy Consumption
	$f_1 = 1/R$	$f_2 = BER$				
Case I	$\omega_1 = 0$	$\omega_2 = 1$	1.294×10^3 bps	79.1×10^{-3}	1.200×10^6 bits	0.5665 Wh
Case IV	$\omega_1 = 0.2$	$\omega_2 = 0.8$	1.411×10^3 bps	88.5×10^{-3}	1.308×10^6 bits	0.5666 Wh
Case III	$\omega_1 = 0.5$	$\omega_2 = 0.5$	1.600×10^3 bps	97.4×10^{-3}	1.483×10^6 bits	0.5666 Wh
Case V	$\omega_1 = 0.8$	$\omega_2 = 0.2$	1.843×10^3 bps	116.8×10^{-3}	1.709×10^6 bits	0.5667 Wh
Case II	$\omega_1 = 1$	$\omega_2 = 0$	1.915×10^3 bps	133.1×10^{-3}	1.776×10^6 bits	0.5668 Wh

schemes, such as M-ary phase-shift keying (MPSK) and quadrature phase-shift keying (QPSK). These techniques combine bits into symbols, and more data can be transmitted in a time instant. Thus, the data rate can be further increased for the same BER.

V. CONCLUSION

This work proposes a mission-based load scheduling algorithm for loads on the CubeSat. The objective is to maximize the data rate and minimize the BER of a communication link between the CubeSat and its base station without exceeding the power and energy limits available. In CubeSat, loads are differentiated into four main categories: TM, MM, TMM, and FL. The operation of TM loads can be shifted in time, whereas MM loads can have adjustable power levels. TMM loads are a combination of both, where both their time and power level are shiftable. FL are loads that require a fixed amount of power and need to be operated during a fixed time instant. Given a combination of different load types, scheduling is crucial to meet the power and energy constraints and avoid energy depletion and mission failure. In this work, the COM system is considered a TMM, whereas the remaining subsystems are considered FL.

A minimization optimization problem is formulated and executed for each day to plan the loads' operation while maintaining the quality of the communication links (data rate and BER) based on the mission requirements. Comparing the results obtained from the unscheduled and scheduled cases proves that the scheduled case results in reduced power consumption by the CubeSat's subsystems since partial power is given to the loads. This is crucial given the power limitations accompanying the small size and volume of the CubeSat. Moreover, the scheduled case shows that the COM system can meet the communication requirements and has relatively reduced BER and increased data rate. Lastly, to investigate the priority considerations, multiple cases were implemented to visualize the impact of the cost function weights on the obtained data rate and BER values. The implementation shows that increasing the weight of a given objective (f_1 or f_2) results in its further minimization. Thus, the priority can be defined by the weights given to the respective objectives in the optimization cost function.

REFERENCES

[1] L. You, K.-X. Li, J. Wang, X. Gao, X.-G. Xia, and B. Ottersten, "Massive MIMO transmission for LEO satellite communication," *IEEE J. Sel. Areas Commun.*, vol. 38, no. 8, pp. 1851–1865, Aug. 2020.

[2] N. Saeed, A. Elzanaty, H. Almorad, H. Dahrouj, T. Y. Al-Naffouri, and M.-S. Alouini, "CubeSat communications: Recent advances and future challenges," *IEEE Commun. Surveys Tut.*, vol. 22, no. 3, pp. 1839–1862, Jul.–Sep. 2020.

[3] I. U. Zaman, A. Eltawil, and O. Boyraz, "Wireless communication technologies in omnidirectional CubeSat crosslink: Feasibility study and performance analysis," *IEEE J. Miniaturization Air Space Syst.*, vol. 2, no. 3, pp. 157–166, Sep. 2021.

[4] O. Khan, M. E. Moursi, H. Zeineldin, V. Khadkikar, and M. A. Hosani, "Comprehensive design and control methodology for DC-powered satellite electrical subsystem based on PV and battery," *IET Renewable Power Gener.*, vol. 14, no. 12, pp. 2202–2210, 2020.

[5] NASA, "2.0 Integrated Spacecraft Platforms," 2022. Accessed: Apr. 2, 2022. [Online]. Available: https://www.nasa.gov/smallsat-institute/sst-soa/integrated-spacecraft-platforms

[6] M. Yaqoob, A. Lashab, J. C. Vasquez, J. M. Guerrero, M. E. Orchard, and A. D. Bintoudi, "A comprehensive review on small satellite microgrids," *IEEE Trans. Power Electron.*, vol. 37, no. 10, pp. 12741–12762, Oct. 2022.

[7] Glenn Research Center, "NASA - Powering the future," 2011. Accessed: Apr. 2, 2022. [Online]. Available: https://www.nasa.gov/centers/glenn/about/fs06grc.html

[8] The European Space Agency, "Kestrel Eye - Satellite Missions - eoPortal Directory," 2017. Accessed: Apr. 2, 2022. [Online]. Available: https://directory.eoportal.org/web/eoportal/satellite-missions/k/kestrel-eye

[9] Gunter's Space Page, "XVI (Link-16)," 2019. Accessed: Apr. 2, 2022. [Online]. Available: https://space.skyrocket.de/doc_sdat/xvi.htm

[10] AAC Clyde Space, "Space missions," 2021. Accessed: Apr. 2, 2022. [Online] Available: www.aac-clyde.space/epic-spacecraft/epic-1u

[11] "Satellites engineered by IAE students, faculty launch on record mission," Univ. South Florida, Tampa, FL, USA, 2021. Accessed: Apr. 2, 2022. [Online]. Available: https://www.usf.edu/engineering/news-room/1-29-2021-usf-iae-arce1-launch.aspx

[12] M. H. Amirioun, F. Aminifar, and H. Lesani, "Towards proactive scheduling of microgrids against extreme floods," *IEEE Trans. Smart Grid*, vol. 9, no. 4, pp. 3900–3902, Jul. 2018.

[13] W. Su, S. S. Yu, H. Li, H. H.-C. Iu, and T. Fernando, "An MPC-based dual-solver optimization method for DC microgrids with simultaneous consideration of operation cost and power loss," *IEEE Trans. Power Syst.*, vol. 36, no. 2, pp. 936–947, Mar. 2021.

[14] A. Kavousi-Fard, A. Zare, and A. Khodaei, "Effective dynamic scheduling of reconfigurable microgrids," *IEEE Trans. Power Syst.*, vol. 33, no. 5, pp. 5519–5530, Sep. 2018.

[15] Y. Li, R. Wang, and Z. Yang, "Optimal scheduling of isolated microgrids using automated reinforcement learning-based multi-period forecasting," *IEEE Trans. Sustain. Energy*, vol. 13, no. 1, pp. 159–169, Jan. 2022.

[16] F. Rodríguez, A. Fleetwood, A. Galarza, and L. Fontan, "Predicting solar energy generation through artificial neural networks using weather forecasts for microgrid control," *Renewable Energy*, vol. 126, pp. 855–864, 2018.

[17] L. Wen, K. Zhou, S. Yang, and X. Lu, "Optimal load dispatch of community microgrid with deep learning based solar power and load forecasting," *Energy*, vol. 171, pp. 1053–1065, 2019.

[18] C. Ahara and J. Rossbach, "The scheduling problem in satellite communications systems," *IEEE Trans. Commun. Technol.*, vol. 15, no. 3, pp. 364–371, Jun. 1967.

[19] B. Sun, W. Wang, X. Xie, and Q. Qin, "Satellite mission scheduling based on genetic algorithm," *Kybernetes*, vol. 39, no. 8, pp. 1255–1261, 2010.

[20] X. Wang, G. Wu, L. Xing, and W. Pedrycz, "Agile Earth observation satellite scheduling over 20 years: Formulations, methods, and future directions," *IEEE Syst. J.*, vol. 15, no. 3, pp. 3881–3892, Sep. 2021.

[21] J. Qi, J. Guo, M. Wang, and C. Wu, "A cooperative autonomous scheduling approach for multiple Earth observation satellites with intensive missions," *IEEE Access*, vol. 9, pp. 61646–61661, 2021.

[22] G. Wun, J. Liu, M. Ma, and D. Qiu, "A two-phase scheduling method with the consideration of task clustering for Earth observing satellites," *Comput. Oper. Res.*, vol. 40, no. 7, pp. 1884–1894, 2013.

[23] L. K. Slongo, S. V. Martínez, B. V. B. Eiterer, T. G. Pereira, E. Bezerra, and K. Paiva, "Energy-driven scheduling algorithm for nanosatellite energy harvesting maximization," *Acta Astronautica*, vol. 147, pp. 141–151, 2018.

[24] R. Darbali-Zamora, E. I. Ortiz-Rivera, and A. A. Rincon-Charris, "Dynamic real-time simulation approach to power management modelling for CubeSat applications," in *Proc. IEEE 46th Photovolt. Spec. Conf.*, 2019, pp. 2792–2797.

[25] X. Wang, J. Atkin, N. Bazmohammadi, S. Bozhko, and J. M. Guerrero, "Optimal load and energy management of aircraft microgrids using multi-objective model predictive control," *Sustainability*, vol. 13, no. 24, 2021, Art. no. 13907.

[26] P. Dobiáš, E. Casseau, and O. Sinnen, "Improving the cubesat reliability thanks to a multiprocessor system using fault tolerant online scheduling," *Microprocess. Microsyst.*, vol. 85, 2021, Art. no. 104312.

[27] K. M. Tsui and S. C. Chan, "Demand response optimization for smart home scheduling under real-time pricing," *IEEE Trans. Smart Grid*, vol. 3, no. 4, pp. 1812–1821, Dec. 2012.

[28] O. Popescu, "Power budgets for CubeSat radios to support ground communications and inter-satellite links," *IEEE Access*, vol. 5, pp. 12618–12625, 2017.

Bayan Hussein (Graduate Student Member, IEEE) received the B.Sc. (Hons.) degree in electrical engineering in 2020 from Qatar University, Doha, Qatar, where she is currently working toward the M.Sc. degree in electrical engineering.

She was a research assistant in a funded project addressing the development of fast electric vehicle battery chargers. Her research interests include power electronics, renewable energy, and power quality.

Ahmed M. Massoud (Senior Member, IEEE) received the B.Sc. (Hons.) and M.Sc. degrees in electrical engineering from Alexandria University, Alexandria, Egypt, in 1997 and 2000, respectively, and the Ph.D. degree in electrical engineering from Heriot-Watt University, Edinburgh, U.K., in 2004.

He supervised several M.Sc. and Ph.D. students at Qatar University. He authored or coauthored more than 130 journal articles in the fields of power electronics, energy conversion, and power quality. He holds 12 U.S. patents. He is currently the Associate Dean for Research and Graduate Studies with the College of Engineering, Qatar University, Doha, Qatar, where he is also a Professor with the Department of Electrical Engineering, College of Engineering. His research interests include power electronics, energy conversion, renewable energy, and power quality.

Dr. Massoud was awarded several research grants addressing research areas such as energy storage systems, renewable energy sources, HVdc systems, electric vehicles, pulsed power applications, and power electronics for aerospace applications.

Tamer Khattab (Senior Member, IEEE) received the B.Sc. and M.Sc. degrees in electronics and communications engineering from Cairo University, Giza, Egypt, and the Ph.D. degree in electrical and computer engineering from The University of British Columbia, Vancouver, BC, Canada, in 2007.

From 1994 to 1999, he was a Development Team Member and then a Development Team Lead with IBM World Trade Corporation, Giza. From 2000 to 2003, he was a senior member of the technical staff with Nokia (formerly Alcatel Canada Inc.), Burnaby, BC, Canada. From 2006 to 2007, he was a Postdoctoral Fellow with The University of British Columbia, where he was involved in prototyping advanced Gb/s wireless local area network (LAN) baseband transceivers. In 2007, he was with Qatar University (QU), Doha, Qatar, where he is currently a Professor of Electrical Engineering. He is also a senior member of the technical staff with Qatar Mobility Innovation Center, Doha, Qatar, a research and development center owned by QU and funded by Qatar Science and Technology Park. He authored and coauthored more than 150 high-profile academic journals and conferences, and has several published and pending patents. His research interests include physical layer security techniques, information-theoretic aspects of communication systems, radar and RF sensing techniques, and optical communication.